ELSEVIER

Journal of Chromatography A, 811 (1998) 105–116

JOURNAL OF CHROMATOGRAPHY A

Monitoring the actual carrier gas flow during large-volume on-column injections in gas chromatography as a means to automate closure of the solvent vapour exit

Thomas Hankemeier*, Sander J. Kok, René J.J. Vreuls, Udo A.Th. Brinkman

Free University, Department of Analytical Chemistry, De Boelelaan 1083, 1081 HV Amsterdam, The Netherlands

Received 6 January 1998; received in revised form 3 March 1998; accepted 3 March 1998

Abstract

Monitoring of the helium flow into a gas chromatograph (GC) by means of an electronic flow meter has been used to optimize and control large-volume on-column injections. The nature of the observed carrier gas flow-rate profiles is discussed in some detail. A rather strong dependence of the evaporation rate on the injection speed was found for injections into a 0.32 mm I.D. retention gap, which can be attributed to the pressure drop along the retention gap when using a solvent vapour exit (SVE). The variation of the evaporation rate with the injection speed was found to be less critical for a 0.53 mm I.D. retention gap. The carrier gas flow-rate profile during the actual injection was used to effect the automated closure of the SVE precisely at the end of the evaporation process. Retention gaps of 0.53 mm I.D. were preferred over 0.32 mm I.D. retention gaps, as 0.53 mm I.D. retention gaps allowed a clearer detection of the end of the evaporation process. Compared with the conventional procedure which involves closure of the SVE at a predetermined time, the present approach is more robust and hardly any optimization is required; it did not cause losses of volatile analytes. The procedure considerably simplifies the use of large-volume on-column injections. Large-volume injections of alkanes were used to study the potential of the large-volume injection–GC system.

Keywords: Large-volume injection; Solvent vapour exit closure; Injection methods; Carrier gas flow; Automation; Evaporation; Alkanes; Ethyl acetate

1. Introduction

The use of large-volume injections (LVI) in gas chromatography (GC), i.e., the injection of a larger aliquot of a sample extract than the conventional 1–5 μl, is attractive from several points of view. The sensitivity (in terms of concentration units) of existing analytical procedures will be increased, which is especially welcome when relatively insensitive detectors such as an infrared detector [1] or certain element channels of an atomic emission detector [2,3] are being used. Next, it allows new strategies in sample preparation, i.e., (i) circumvention of solvent evaporation which often is the final step in off-line procedures; (ii) miniaturization of existing procedures, which will result in the use of smaller sample and extraction solvent volumes, and/or (iii) on-line coupling of sample preparation and GC analysis.

Several concepts for the injection of large sample volumes into a GC have been reported. Two tech-

*Corresponding author. Present address: TNO Institute for Nutrition and Food Research, Analytical Sciences Division, Utrechtseweg 48, 3704 HE Zeist, The Netherlands.

0021-9673/98/$19.00
PII: S0021-9673(98)00193-9

niques can be used for most types of application, i.e., large-volume on-column [4–6] and programmed temperature vaporizer (PTV) [7,8] injection. If the sample extract is not too dirty, on-column injection is preferred, because it allows the determination of volatile as well as high-boiling analytes without any hardware modifications such as cooling with CO_2, which is necessary for PTV injection.

With large-volume on-column injections, the solvent is injected into a retention gap which is mounted in front of the analytical column. An early solvent vapour exit (SVE) is generally used to increase the evaporation rate and to protect the detector from excessive amounts of solvent vapour [9]. In order not to loosen the volatile analytes, the SVE exit has to be closed at a predetermined time, i.e. just before the evaporation of the last part of the solvent. This point in time can be determined by monitoring the effluent leaving the SVE by flame or flame ionization detection (FID) at high attenuation ([10], p. 127). Alternatively, the closure time of the SVE can be derived from a series of injections performed at different closure times, viz. by determining at which closure time the volatile analytes are quantitatively recovered [4]. However, after optimization, slight changes of, for example, the carrier gas pressure, the injection speed and/or the injected volume due to the presence of, e.g., a small bubble in the syringe of an autosampler, will easily result in too late a closure and, consequently, loss of volatile analytes. In practice, even the exchange of a press-fit can influence the optimum conditions or, in other words, the procedures are not really robust.

Obviously, it is desirable to make optimization less time-consuming or even superfluous. One instrument manufacturer developed a software package which calculates appropriate parameters for a fixed set-up [5]. However, the algorithm of the software is not described, and only one type of retention gap can be used. In principle, it is also possible to calculate the evaporation rate for a specific instrument set-up [11]. However, as such calculations of the evaporation rate are only approximately correct, the closing of the SVE still has to be optimized. Obviously, automated closure of the SVE at the correct moment is highly desirable.

In the present study, the changes in the actual flow-rate of the carrier gas during and at the end of the evaporation process were used to optimize and control large-volume on-column injections. The helium flow into the GC was measured by means of an electronic flow meter. Relevant theoretical aspects, such as the influence of the internal diameter of the retention gap, the head pressure and injection temperature and the injection speed, were studied in detail. The goal was to automate the closure of the SVE at the proper moment in time on the basis of the flow-rate profile of the carrier gas during injection and evaporation. The performance of the new concept was compared with that of the conventional procedure.

2. Experimental

2.1.1. Chemicals

Ethyl acetate and hexane (both analytical-reagent grade, J.T. Baker, Deventer, The Netherlands) were distilled before use. A 1 μg/μl stock solution of several *n*-alkanes in the C_8–C_{20} range (cf. Table 3) was prepared in *n*-hexane and stored in the dark at 4°C. For large-volume on-column injections, it was diluted to a concentration of 0.5 ng/μl.

2.1.2. Set-up of large-volume injection–GC system

The large-volume injection–GC system (Fig. 1)

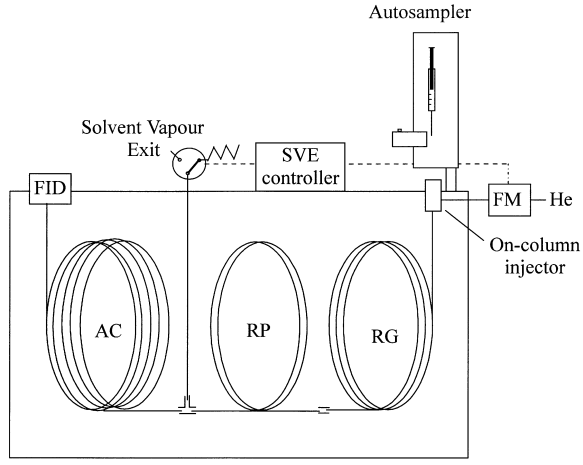

Fig. 1. Set-up of the large-volume injection–GC system. Abbreviations: AC, analytical column; RP, retaining precolumn; RG, retention gap; FM, flow meter; He, helium; SVE, solvent vapour exit.

consisted of a Carlo Erba Series 8000 gas chromatograph equipped with an on-column injector and an FID-80 (CE Instruments, Milan, Italy). A Model F101D-HA mass flow meter (Bronkhorst, Ruurlo, The Netherlands) was installed between the pressure regulator and the on-column injector; the flow was determined by means of thermal conductivity and was independent of the pressure. A 3-m diphenyltetramethyldisilazane-deactivated retention gap (DPTMDS, 0.53 mm I.D.; BGB Analytik, Zurich, Switzerland) was connected to a 2-m retaining precolumn and a 28-m analytical column (both DB-XLB, 0.25 mm I.D., film thickness 0.25 μm; J&W, Folsom, CA, USA) via a press-fit connector and a Y-piece, respectively. The SVE, an electronically controlled 6-port valve (Valco Instruments, Houston, TX, USA), was connected to the T-piece. The SVE was either controlled by a pre-programmed remote event of the GC, or by the SVE controller, which was developed during the present project. The FID detector settings for the acquisition of chromatograms were chosen according to the manual (air, 350 ml/min; hydrogen, 25 ml/min). The standard boiling point of a solvent was used as the initial GC temperature, i.e. 77°C for the injection of ethyl acetate and 69°C for hexane. Helium 5.0 (Hoekloos, Schiedam, The Netherlands) was used as carrier gas; unless it is stated differently in the text, the head pressure was 110 kPa.

Unless stated differently, injections were performed with an automated syringe pump (Harvard Apparatus 22, South Natick, MA, USA) using a 500-μl syringe with a PTFE-coated plunger. After filling and mounting it on the Harvard pump, the sample was transferred to the on-column injector via a stainless-steel needle (O.D. 0.25 mm).

For injections with the AS 800 autosampler (CE Instruments), a 250-μl syringe with a PTFE plunger and an injection needle of 0.5 mm O.D. were used. The appropriate settings for the autosampler were programmed by means of Chromcard Ver. 1.33 (CE Instruments). For injections with the AS 800 autosampler the injection speed was 2 μl/s.

After the automated closure of the SVE by the SVE controller, the temperature programme of the GC was started with a delay of 2.5 min. The temperature was increased to 280°C at 20°C/min, and held at 280°C for 1 min.

2.1.3. FID monitoring of solvent peak

Next to the carrier gas flow-rate profile, the solvent peak was monitored, viz. with the FID. A press-fit splitter was connected to the retention gap. A 0.2 m×0.1 mm I.D. fused-silica restriction was used to direct about 0.5% of the gas flow to the FID. The other outlet of the T-splitter was connected to 0.9 m of a 0.32 mm I.D. retention gap. In order to record the whole solvent peak, the air flow of the FID was increased to 1500 ml/min by removing the restriction in front of the pressure controller, and the range was set to 10^3.

2.1.4. Automated detection of end of evaporation and SVE closure

A microprocessor-based SVE controller with a small keyboard and LCD display was constructed and a programme written in C to actuate the closure of the SVE. The helium flow was registered by the programme every 200 ms via an A/D converter. Communication with the AS 800 autosampler and GC instrumentation was achieved by means of contact closure events.

When ready for a next run, the GC instrumentation gave a start signal to the AS 800 autosampler. When the autosampler was ready for injection, a signal was given to the SVE controller to open the SVE. After a delay time of 0.05 min, the injection was started. The syringe was removed 0.05 min after completion of the injection. After an additional delay time of 0.05 min to allow stabilization of the helium flow, monitoring of the helium flow by the SVE controller was initiated. As soon as the first derivative of the helium flow [which was calculated by subtracting the one-but-last from the last value] exceeded a preset threshold value, the SVE was closed and the GC run started. All relevant parameters, i.e. the pre-injection delay time, the injection time, the post-injection delay time and the threshold value, could be programmed in the SVE controller and were stored in its memory. The closure times of the SVE were stored in the memory of the SVE controller and could be displayed for 50 injections.

3. Results and discussion

In order to achieve the goals outlined in Section 1,

two major aspects were studied. Firstly, the helium flow-rate and the solvent evaporation profile for large-volume injections recorded for 0.32 and 0.53 mm I.D. retention gaps were compared. Next, the usefulness of monitoring the helium flow to achieve automated closure of the SVE was studied and the results compared with those of conventional procedures.

3.1. Helium flow-rate profile and solvent evaporation profile for large-volume injections

Injection of ethyl acetate into a retention gap was studied by monitoring the helium flow into the on-column injector of the GC with a flow meter, while the solvent vapour leaving the retention gap was monitored by FID. To this end, the flow at the outlet of the retention gap was split, and only about 0.5% of the effluent was directed to the FID system. This type of injection resembles a large-volume injection with the SVE open and in the absence of a retaining precolumn. The injection syringe remained in the injector during solvent evaporation after the injection had been completed. Injections were done with the Harvard pump.

The influence of parameters such as the internal diameter of the retention gap, injection speed and head pressure on the helium flow-rate profile and the profile of the solvent peak were studied. The main focus was on the use of the helium flow-rate profile to detect the start and end of the evaporation process.

3.1.1. Diameter of retention gap

Injections of 0.33 min into a 4 m×0.53 mm I.D. retention gap were carried out at a head pressure of 46 kPa. Using the set-up described (see Section 2), a helium flow-rate of 21.9 ml/min was obtained.

For all injection speeds studied, the helium flow decreased rapidly at the very moment that solvent entered the retention gap. The helium flow-rate profiles in the top part of Fig. 2 show several typical examples, which were recorded under different conditions. When injecting at a speed below the evaporation rate, e.g. 100 μl/min, the helium flow sharply increased at the end of the injection (Fig. 2A, full-drawn line). As was to be expected, when injecting at a speed above the evaporation rate, e.g. 160 or 260 μl/min (Fig. 2B and Fig. 2C; full-drawn lines), the helium flow-rate increase was delayed: it sharply increased 0.12 min or 0.55 min after the end of the injection (the arrows in Fig. 2 indicate completion of the injection), respectively, because the residual 10

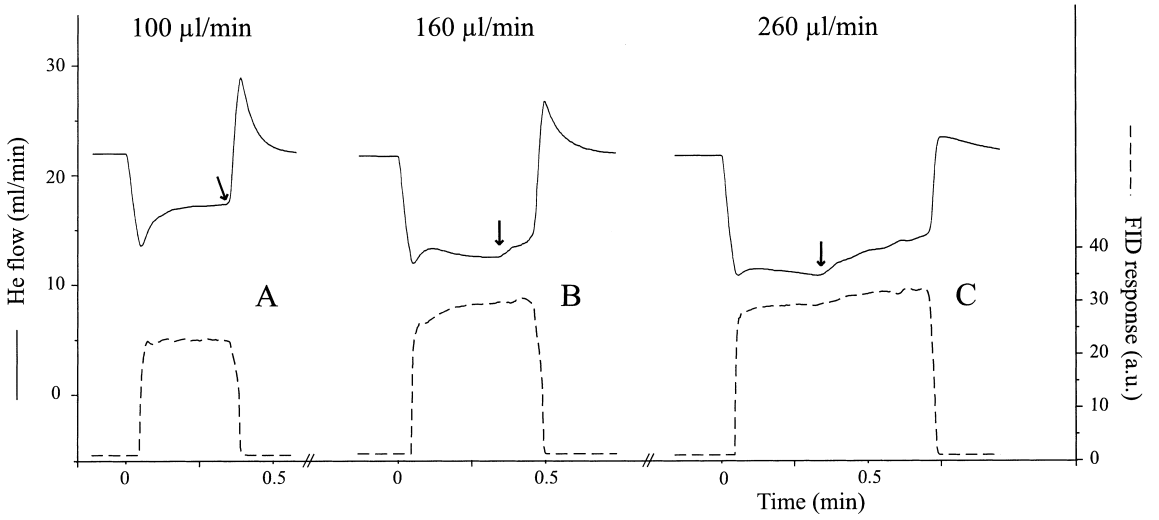

Fig. 2. Helium flow-rate profile (full-drawn lines) and solvent peak profiles (broken lines) for injections of ethyl acetate into a 0.53 mm I.D. retention gap. Injection time, 20 s; injection speed: (A) 100 μl/min, (B) 160 μl/min, and (C) 260 μl/min. As the evaporation rate was determined to be 130 μl/min, with the latter two injections 10 μl and 43 μl were left as solvent film in the retention gap, respectively. The syringe was not removed from the injector after the injection. The end of the injection is indicated by an arrow.

or 43 μl of solvent film left in the retention gap at the end of the injection had to evaporate.

The solvent peak which was recorded simultaneously by FID began to show up 0.05 min after the start of an injection (Fig. 2, broken lines) because of the delay due to the transport of the solvent vapour from the point of injection through the retention gap and restriction to the FID system. The solvent peak decreased abruptly 0.01–0.03 min after the increase of the helium flow at the end of the evaporation process. This delay is shorter than that at the start of the injection because, at the end of the evaporation process, evaporation occurs further down in the retention gap than at the start of an injection. Consequently, the width of the solvent peak recorded by FID is somewhat shorter than the signal recorded by the helium flow meter. The more solvent is left in the retention gap at the end of the injection, the further does the solvent film extend into the retention gap, and the shorter will be the second delay time (since the small difference cannot easily be seen from Fig. 2, see especially discussion of Table 1).

Next, injections of 0.33 min were carried out into a smaller-bore, i.e. a 5.1 m×0.32 mm I.D. retention gap (connected to a 0.9 m×0.32 mm I.D. capillary) at a head pressure of 63 kPa. With the transfer line inserted, a helium flow-rate of 6.5 ml/min was obtained.

The helium flow-rate profiles in the top part of Fig. 3 show sharp decreases and increases in the helium flow at the start and end of the evaporation process, respectively; these are comparable to those of Fig. 2. In the present example, about 12 μl and 39 μl were left in the retention gap at the end of the injection, so that the helium flow started to increase with a delay of 0.30 min (Fig. 3A) and 0.60 min (Fig. 3B), respectively. The solvent peak recorded by FID again started to show up 0.05 min after the decrease of the helium flow. However, different from the injections into a 0.53 mm I.D. retention gap, the helium flow-rate changed significantly during the injection and evaporation process. The large increase of the helium flow after the injection had been completed was especially remarkable (cf. Fig. 3B, arrow indicates completion of injection). It will be discussed in more detail in Section 3.1.3.

3.1.2. Injection speed

In order to check if the evaporation rate was independent of the position of the solvent film in the retention gap, two 36-μl injections were carried out at 180 and 360 μl/min into a 0.53 mm I.D. retention gap, so that 10 μl or 23 μl of solvent were left in the retention gap at the end of the injection (Table 1). The evaporation as indicated by the helium flow-rate took 0.48 and 0.49 min. In other words, the evaporation rate depended only slightly on the position and length of the solvent film in the 0.53 mm I.D. retention gap. However, for the same two injections the solvent peak widths recorded by FID showed a somewhat larger increase, viz. from 0.50 min to 0.52 min. As explained above, this is due to the fact that the farther down the last portion of solvent is in the retention gap at the end of the evaporation process, the shorter the hold-up time to the FID system will be. This suggests that monitoring the injection by

Table 1
Characteristics of solvent evaporation for 36-μl injections into a 0.53 and 0.32 mm I.D. retention gap using different injection speeds[a]

Retention gap	Injection speed (μl/min)	Solvent film in RG[b] (μl)	Evaporation time (min)	
			He flow	FID[c]
0.53 mm I.D.	360	23	0.48±0.01	0.50±0.01
	180	10	0.49±0.01	0.52±0.01
0.32 mm I.D.	360	32	0.68±0.02	0.59±0.02
	180	27	0.76±0.02	0.71±0.02
	60	6	0.84±0.02	0.82±0.02

[a] Set-up and head pressure same as for injections shown in Figs. 2 and 3; syringe left in injector after injection.
[b] Amount of solvent left in retention gap (RG) at end of injection, V_s, calculated from: $V_s=(v_{inj}-v_{evap})\times t_{inj}$ with v_{inj}, injection speed; t_{inj}, injection time, v_{evap}, evaporation rate (determined from repetitive injections of pure solvent at increasing injection speed [10]).
[c] Solvent peak width at half maximum.

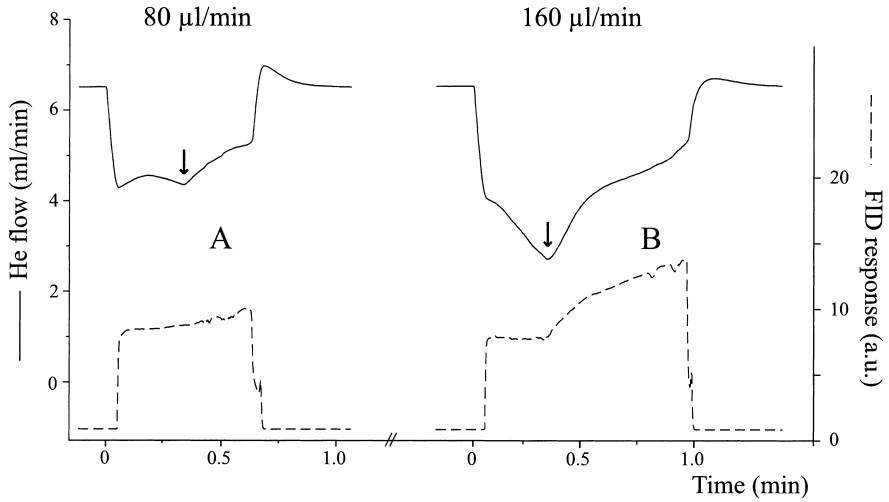

Fig. 3. Helium flow-rate profile (full-drawn lines) and solvent peak profiles (broken lines) for injections of ethyl acetate into a 0.32 mm I.D. retention gap. Injection time, 20 s; injection speed: (A) 80 µl/min, and (B) 160 µl/min, leaving a film of 12 µl and 39 µl in the retention gap after injection, respectively. The syringe was not removed after injection. The end of the injection is indicated by an arrow.

means of the helium flow will be more precise than with FID, because the helium flow will start to increase immediately after the evaporation process is completed, irrespective of the position of the last drop of solvent in the retention gap.

The situation was, however, rather different for injections into a 0.32 mm I.D. retention gap. When varying the injection speed of the 36-µl injections causing from 6 to 32 µl of solvent to be left in the retention gap after injection, the duration of the evaporation as monitored by means of the helium flow changed significantly, i.e. from 0.68 min to 0.84 min and, if monitored by FID, even more, i.e. from 0.59 min to 0.82 min (Table 1). Obviously, for the 0.32 mm I.D. retention gap the evaporation rate depends rather strongly on the position of the solvent film.

3.1.3. Discussion

The above observations can be explained by taking into account the dependence of the helium flow, F_{He}, on the following three parameters: (i) the ratio of the vapour pressure of helium and the solvent used, (ii) the viscosity of the gas mixture, and (iii) the flow resistance of the system, according to [12]:

$$F_{He} = y_{He}(600\pi r^4 6\eta_m L) \times [(p_i^2 - p_o^2)/p_o](p_o/p_{ref})(T_{ref}/T) \quad (1)$$

with: F_{He}, flow-rate of helium, ml/min; y_{He}, mole fraction of helium; r, internal radius of retention gap, cm; η_m, viscosity of the helium and solvent gas mixture calculated according to Wilke's approximation, Poise [11,12]; L, length of retention gap, cm; p_i and p_o, pressures at inlet and outlet of the retention gap, Pa; p_{ref}, reference pressure, $1.0^1 \times 10^5$ Pa; T, column temperature, K; T_{ref}, reference temperature, 298.15 K. Ideal gas behaviour of the solvent vapour and saturation of the gas phase with solvent vapour are assumed. A possible decrease of the retention gap temperature due to the evaporating solvent was not taken into account. Because the molar fraction, the viscosity and the solvent film thickness may vary along the length of the retention gap (see discussion below), Eq. (1) is only valid for an infinitesimal part of the retention gap, and we therefore had to calculate the helium flow iteratively. In addition, the pressure drop due to the insertion of the injection needle had to be taken into account.

At the start of the injection, the mole fraction of helium and the viscosity of the gas mixture start to change. The mole fraction of helium starts to decrease, and the viscosity of the mixture of helium

and solvent vapour will become lower than that of pure helium, because the viscosity of the solvent vapour, i.e. ethyl acetate or hexane, is significantly lower than that of helium. Eq. (1) reveals that in most cases the helium flow will be lower during the injection and evaporation process than prior to the injection. (An increase of the helium flow will occur only if a solvent with a very low-viscosity vapour is used at a temperature much below the boiling point.) The helium and solvent vapour flows are also reduced by the increase of the restriction of the retention gap caused by the presence of the solvent film. To give an example, for the injection of ethyl acetate into a 0.53 mm I.D. retention gap, a flooded zone of 5.6 cm/μl has been calculated [13], which corresponds with an average film thickness of about 11 μm. According to Eq. (1), a decrease of the internal diameter by 22 μm would result in a decrease of the flow by 15% for a retention gap of 0.53 mm I.D. and 25% for one of 0.32 mm I.D.

When injecting at a speed below the evaporation rate, neither the mole fraction of helium nor the viscosity of the helium and solvent gas mixture will change significantly during injection, because no solvent film of significant length is created in the retention gap. Therefore, the helium flow-rate and, also, the height of the solvent peak will be essentially constant during injection (Fig. 2A). However, we invariably observed a noticeable dip of the helium flow-rate at the very beginning of the injection, and a rapid increase occurred at the end of the evaporation before the flow returned to its initial value. These dips and peaks of varying intensity (cf. Fig. 2C and Fig. 3A) are probably connected with the rapid change of the contents of the retention gap, which occurs when part of the helium is suddenly replaced by solvent vapour, or vice versa, and the viscosity suddenly changes dramatically.

If the injection speed is above the evaporation rate, the mole fraction of helium, the viscosity of the gas mixture, and the restriction caused by the solvent film, keep changing during injection and evaporation, which further complicates matters and causes the rather complex helium flow-rate and solvent peak profiles of Fig. 2B, Fig. 2C and Fig. 3. In that part of the retention gap in which there is a solvent film, the vapour pressure of the solvent remains constant (Fig. 4, Trace B), and the ratio (helium pressure/solvent vapour pressure) (Fig. 4, Trace C) will decrease due to the total pressure drop along the retention gap (Fig. 4, Trace A). Consequently, the viscosity will also change in that part of the retention gap. However, from the front of the solvent film to the SVE, the ratio (helium pressure/solvent vapour pressure) does not change any more (Fig. 4, Trace C) and the viscosity will therefore remain constant.

For an injection speed higher than the evaporation rate, a further increase will cause the solvent film at the injection point to become thicker and to reach farther into the retention gap. During the injection, the helium flow will continue to decrease as the film reaches farther into the retention gap, and this decrease will be larger for higher injection speeds. To quote a few examples, Eq. (1) predicts that for the 80-μl/min injection of Fig. 3A into a 0.32 mm I.D. retention gap the helium flow will decrease from 6.8 ml/min to 4.7 ml/min at the start of the injection (decrease from 6.5 to 4.8 ml/min experimentally measured) and to 4.2 ml/min at the end of the injection (4.4 ml/min measured) (Table 2). For the 160-μl/min injection of Fig. 3B, a decrease to 3.1 ml/min at the end of the injection is predicted (2.7 ml/min measured). After the injection, the solvent film is pushed farther into the retention gap [13,14] and its thickness becomes more uniform and, of course, also starts to decrease. The solvent evaporates mainly from the rear end till just prior to the end of the evaporation only a short thin film of solvent is left. Both effects result in an increase of the helium flow (cf. Eq. (1)). As an example, just prior to the end of the evaporation of the 160-μl/min injection of Fig. 3B, the helium flow-rate is predicted to be 5.2 ml/min (5.3 ml/min measured). Table 2 provides more details concerning these calculations.

For injections into the 0.53 mm I.D. retention gap (cf. Fig. 2), Eq. (1) predicts the change of the helium flow between the sharp decrease at the start of the injection and the sharp increase at the end of the evaporation to be less than for the 0.32 mm I.D. retention gap. To quote an example, the helium flow of the 260-μl/min injection of Fig. 2C was calculated to decrease at the start of the injection from 22.4 ml/min to 13.2 ml/min (decrease from 21.9 ml/min to 11.9 ml/min measured). The flow at the end of the injection was calculated to be 11.8 ml/min (10.9 ml/min measured), and that just prior to

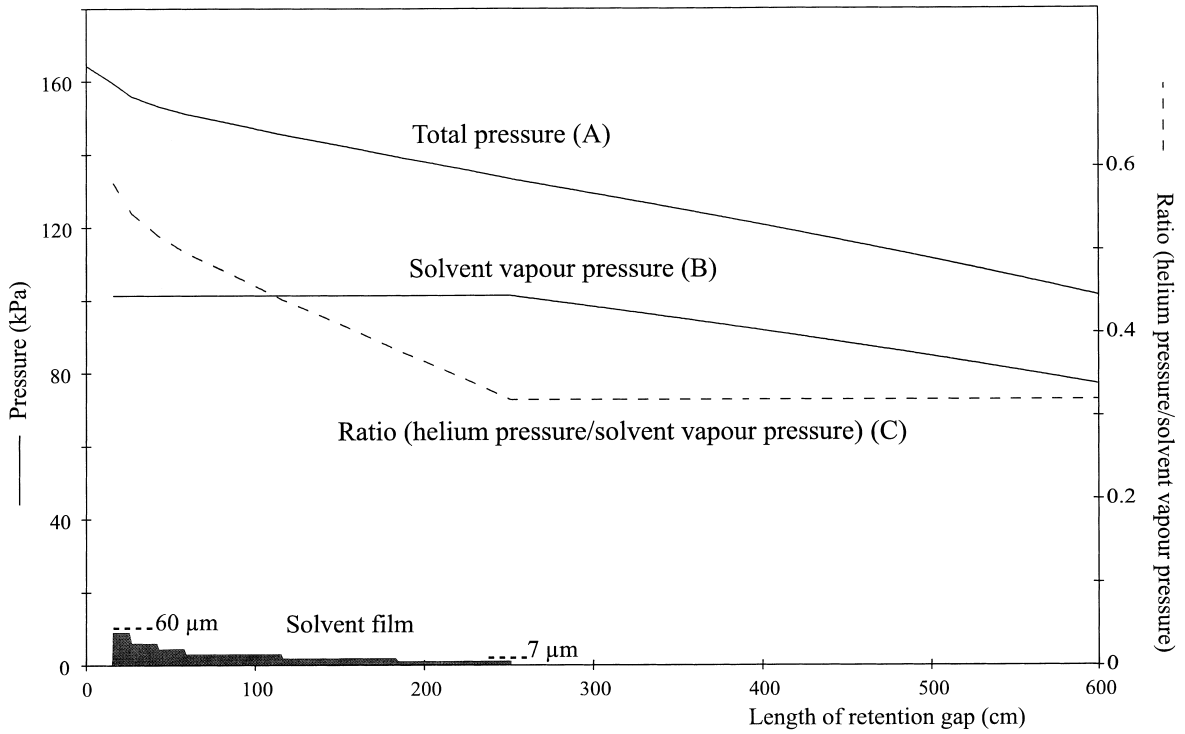

Fig. 4. Theoretical profile of (A) the total pressure, (B) the solvent vapour pressure, and (C) the ratio (helium pressure/solvent vapour pressure) in the retention gap at the end of the 160-µl/min injection of Fig. 3B. The profiles were (iteratively) calculated by means of Eq. (1) using the solvent film distribution as shown. For more details, see text and notes of Table 2.

the end of the evaporation to be 13.9 ml/min (14.6 ml/min measured).

The predicted and experimentally measured helium flow-rates agree rather satisfactorily, and the up to 15% differences can be primarily attributed to the approximations briefly mentioned above when introducing Eq. (1) (also see notes of Table 2).

In other words, the calculated values predict the changes of the helium flow-rate during the injection rather well, notably the sharp decrease at the start of the injection, the slower changes during the injection and evaporation process and the final sharp increase when evaporation is complete. The fact that the change of the helium flow-rate during injection and evaporation is smaller for a 0.53 mm I.D. than for a 0.32 mm I.D. retention gap is also correctly predicted.

As with the helium flow-rate, the evaporation rate of the solvent depends on the ratio (helium pressure/solvent vapour pressure), the viscosity of the gas mixture and the restriction caused by the solvent film in the retention gap. As these parameters keep changing during injection and evaporation if injection is done at a speed above the evaporation rate, the evaporation rate depends on the injection speed and the amount of solvent injected. As demonstrated for the helium flow-rate, Eq. (1) predicts this dependence to be larger for injections into a 0.32 mm I.D. than into a 0.53 mm I.D. retention gap. The larger variation of the evaporation rate with the injection speed for injections into a 0.32 mm I.D. was confirmed by the experiments of Table 1. This aspect will be discussed in more detail in the near future [15].

3.2. Automated closure of the SVE

Since it was our intention to use the sharp increase of the flow-rate at the end of the evaporation process for the automated closure of the SVE, we compared

Table 2
Calculation of helium flow-rates at various moments during injections into a 0.32 mm I.D. (cf. Fig. 3) or a 0.53 mm I.D. (cf. Fig. 2) retention gap[a]

Retention gap (mm I.D)	Situation	He flow (ml/min)	
		Calculated	Measured
0.32	*Prior to injection*[b]	6.8	6.5
	80 μl/min (Fig. 3A)		
	Start of injection	4.7	4.8[c]
	End of injection	4.2	4.4
	End of evaporation	4.8	5.2
	160 μl/min (Fig. 3B)		
	Start of injection	4.5	4.1[c]
	End of injection	3.1	2.7
	End of evaporation	5.2	5.3
	After end of evaporation[b]	6.8	6.5
0.53	*Prior to injection*[b]	22.4	21.9
	160 μl/min (Fig. 2B)		
	Start of injection	13.4	14.1[c]
	End of injection	13.1	12.6
	End of evaporation	13.4	14.3
	260 μl/min (Fig. 2C)		
	Start of injection	13.2	11.9[c]
	End of injection	11.8	10.9
	End of evaporation	13.9	14.6
	After end of evaporation[b]	22.4	21.9

[a] Helium flow calculated by means of Eq. (1). Solvent film thickness distributions used for calculations were estimated, as no exact experimental data were available. Position of last portion of solvent just prior to end of evaporation was calculated by multiplying amount of solvent left in retention gap at end of injection (cf. Table 1, note b) with flooded zone (expressed in cm/μl; 5.6 and 9.3 cm/μl for 0.53 and 0.32 mm I.D. retention gaps, respectively), assuming a constant flooded zone. Front of solvent film at end of injection was assumed to be at 70% of distance into retention gap of position of last portion of solvent just prior to end of evaporation (cf. above; comparable data found in [13]). As an example, estimated solvent film thickness distribution at end of injection of Fig. 3B is given in Fig. 4. Solvent film thickness distributions for other injections were obtained in a similar way as that of Fig. 3B; data available from the authors upon request.
[b] 15 cm of 0.25 mm O.D. needle of syringe inserted into retention gap.
[c] Negative peak at start of injection is ignored.

the loss of volatiles occurring when (i) closing the SVE on the basis of the helium flow-rate profile, and (ii) using a pre-set closure time at which not all solvent had evaporated as yet. A retention gap of 0.53 mm I.D. was preferred over one with 0.32 mm I.D., because the helium flow-rate profile then is simpler and the completion of the evaporation process, consequently, can be detected more easily.

Fig. 5 shows that using the first derivative of the helium flow-rate profile (Trace A) is a simpler alternative than using the profile itself (Trace B) for the (automated) indication of the end of the evaporation process because of the better stability of the signal during evaporation, and the shaper final increase. In a first experiment the SVE was manually closed at the end of the evaporation process as indicated by the helium flow-rate profile. Since a comparison of the results obtained for injections of *n*-alkanes (C_8–C_{20}) in ethyl acetate made under these conditions and of injections made when the SVE was closed 0.05–0.1 min prior to completion of the evaporation process did not indicate any loss of even C_9 or C_{10}, a microprocessor-based controller was built to monitor the flow to automate the closure of the SVE.

The SVE was (automatically) closed when the first derivative exceeded a pre-set threshold value; the influence of the choice of this threshold value was studied using 30-μl injections of *n*-alkanes in ethyl acetate at 120 μl/min and threshold values from 10 to 80 ml/min^2 [the evaporation rate was found to be 47 μl/min]. This resulted in a closure of the SVE

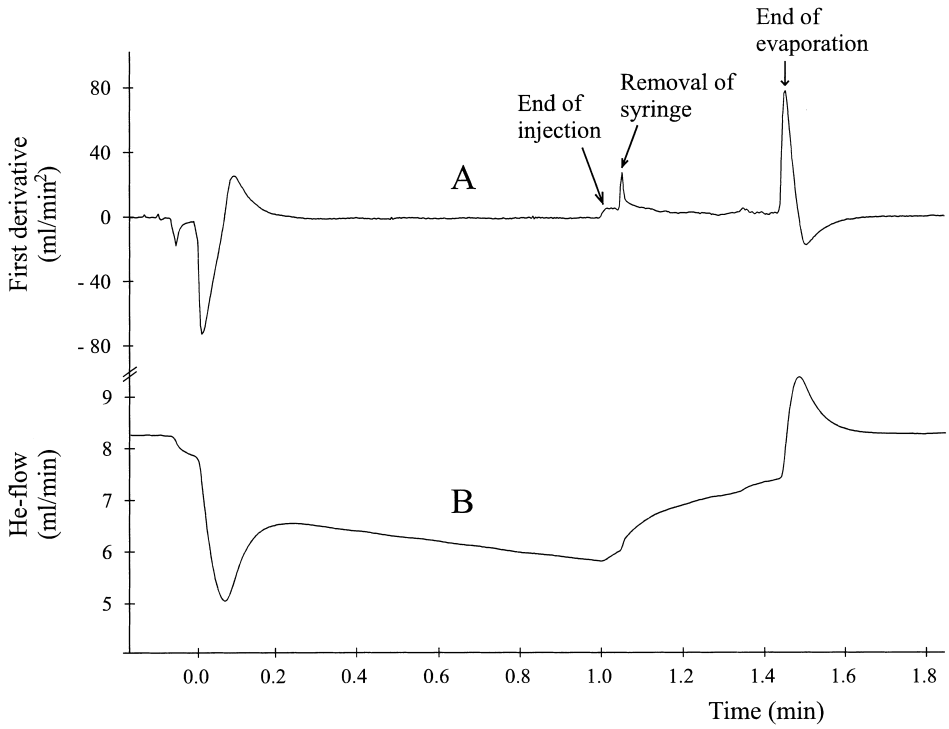

Fig. 5. Helium flow-rate profile (B) and its first derivative (A) for a 60-μl injection of *n*-hexane in a 6 m×0.32 mm retention gap connected to a 1.5 m×0.32 mm retaining precolumn. Injection started at 0 min, needle inserted into injector 0.05 min before start of injection, and removed 0.05 min after end of injection; SVE left open all the time.

0.01–0.02 min (for 10–50 ml/min^2) or 0.04 min (for 80 ml/min^2) after evaporation was completed, i.e. after the helium flow started to increase. In all cases, the recoveries of the relatively volatile C_8–C_{11} *n*-alkanes were between 94 and 98% compared with a 30-μl injection with which the SVE was closed 0.07 min before evaporation was complete. Not unexpectedly, when the SVE was closed 0.15 min too late, the volatile *n*-alkanes up to C_{14} were completely lost. As a compromise between too early closure and late closure (or no closure at all), a threshold value of 30 ml/min^2 was selected for further work. Monitoring of the first derivative was started 0.05 min after withdrawal of the syringe, because the helium flow by then was stable again after the peak caused by the withdrawal of the syringe (cf. Fig. 5, Trace B). It should be mentioned that, when starting monitoring of the flow only with a delay after the end of injection, some solvent has still to be left in the retention gap at the moment monitoring of the helium flow is started. With other words, the injection speed has to be higher than the evaporation rate to allow automated closure. However, when monitoring is started immediately at the end of the injection, i.e. without a delay, automated closure also occurs when the injection speed is equal to or slightly below the evaporation rate.

The reliability of the automated SVE closure was tested by performing 42 30-μl injections of a standard solution of *n*-alkanes in *n*-hexane by means of the GC autosampler. All *n*-alkanes from *n*-octane on showed up in the GC–FID chromatogram (Fig. 6). Comparison with an injection with which the SVE was closed 0.05 min before the end of the evaporation showed that they were quantitatively recovered (recoveries, 98-101%; cf. Table 3). The relative standard deviation (R.S.D.) of the SVE closure time was 0.09% at an average SVE closure time of 0.48 min, and the R.S.D. values of the peak areas were quite good (1–4.5%, cf. Table 3). One should add

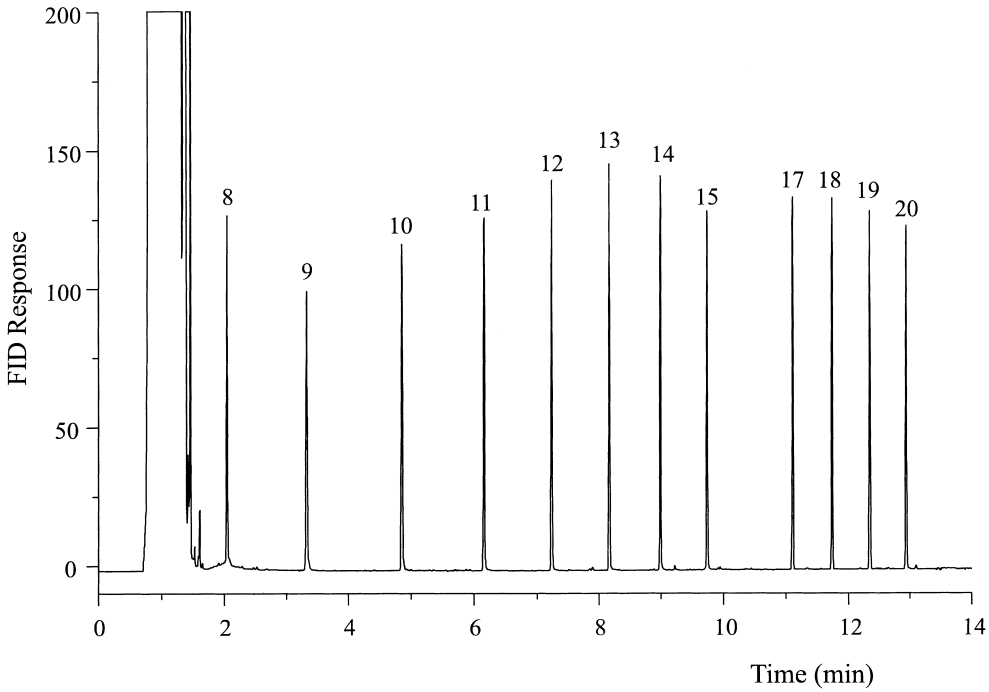

Fig. 6. GC–FID chromatogram of a 30-μl injection of *n*-alkanes in *n*-hexane. The closure of the SVE was automated by means of a laboratory-made microprocessor-based controller. For more details, see text.

that, even if the injection or evaporation process would show a poorer precision than in the present instance, the SVE controller will still close the SVE just at the end of the evaporation process. This will cause the retention times to remain constant and no loss of volatiles will occur, whereas with closure at a preprogrammed time, retention times may well shift and/or volatile analytes may be lost.

During over 300 injections, no automated closure was ever observed which occurred too early due to changes of the helium flow during evaporation of the solvent.

Table 3
Recoveries and repeatability of peak areas of several *n*-alkanes for 30-μl injections in *n*-hexane using automated closure of the SVE

Compound	Recovery[a] (%)	R.S.D. (%, $n=42$)
C_8	99	3.2
C_9	98	2.9
C_{10}	101	3.1
C_{11}	100	4.1
C_{15}	99	3.4
C_{17}	99	4.3
C_{18}	98	0.9
C_{19}	100	0.8
C_{20}	98	1.0

[a] The recoveries were calculated by using as a reference a 30-μl injection with which the SVE was closed by the GC programme rather than the SVE controller 0.1 min prior to completion of the evaporation process. For further details, see text.

4. Conclusions

Monitoring of the helium flow allows the (automated) control of large-volume on-column injections. The end of the evaporation process can be detected (as a sharp helium flow increase) without any delay due to a hold-up time. Actually, for nearly all large-volume injections into 0.32 or 0.53 mm I.D. retention gaps, the helium flow will sharply decrease at the start of the injection and sharply increase when evaporation is complete. This is especially true for a 0.53 mm I.D. retention gap which was therefore selected for use in the automated SVE closure set-up.

Pre-optimization or calculation of a fixed time for the SVE closure now is superfluous. In addition, even when the evaporation time slightly changes due to, e.g., small changes of the injection speed or injection volume, the SVE will be closed just in time without undue loss of volatiles or a significant change of the solvent peak width at the detector. The latter aspect is important when working with a mass-selective detector, because the delay time for switching on the filament can now be kept constant.

Implementation of (automated) helium flow monitoring is an important step towards a self-optimizing large-volume on-column injection system. A self-optimizing system is to be preferred to a system in which all parameters are pre-optimized (or calculated), because the latter is rather vulnerable if small changes in the experimental conditions or set-up occur.

Acknowledgements

The authors thank the European Union for their support to Th. Hankemeier via a Human Capital and Mobility grant (No. EV5V-CT-93-5225). They are also grateful to Lex van der Gracht (Electronic Workshop, Free University) for constructing the SVE controller.

References

[1] Th. Hankemeier, H.T.C. van der Laan, J.J. Vreuls, M.J. Vredenbregt, T. Visser, U.A.Th. Brinkman, J. Chromatogr. A 732 (1996) 75.
[2] F.D. Rinkema, A.J.H. Louter, U.A.Th. Brinkman, J. Chromatogr. A 678 (1994) 289.
[3] H.-J. Stan, M. Linkerhägner, J. Chromatogr. A 727 (1996) 275.
[4] S. Ramalho, Th. Hankemeier, M. de Jong, U.A.Th. Brinkman, J.J. Vreuls, J. Microcol. Sep. 7 (1995) 383.
[5] F. Munari, P.A. Colombo, P. Magni, G. Zilioli, S. Trestianu, K. Grob, J. Microcol. Sep. 7 (1995) 403.
[6] A. Venema, J.T. Jelink, J. High-Resolut. Chromatogr. 19 (1996) 234.
[7] H.G.J. Mol, H.-G. Janssen, C.A. Cramers, U.A.Th. Brinkman, J. High-Resolut. Chromatogr. 18 (1995) 19.
[8] H.G.J. Mol, H.-G. Janssen, C.A. Cramers, U.A.Th. Brinkman, Trends Anal. Chem. 15 (1996) 206.
[9] K. Grob, H.-G. Schmarr, A. Mosandl, J. High-Resolut. Chromatogr. 12 (1989) 375.
[10] K. Grob. In: W. Bertsch, W.G. Jennings, P. Sandra (Eds)., On-line Coupled LC–GC, Hüthig, Heidelberg, 1991, p. 127.
[11] J. Staniewski, K. Alejski, Poster presented at 18th Intl. Symp. on Capillary Chromatography, Riva del Garda, 1996.
[12] R.C. Reid, J.M. Prausnitz, Th.K. Sherwood, The Properties of Gases and Liquids, 3rd ed., McGraw-Hill, New York, 1977.
[13] Th. Hankemeier, A.J.G. Mank, J.J. Vreuls, U.A.Th. Brinkman, in preparation.
[14] K. Grob Jr., G. Karrer, M.-L. Riekkola, J. Chromatogr. 334 (1985) 129.
[15] Th. Hankemeier, S.J. Kok, J.J. Vreuls, U.A.Th. Brinkman, in preparation.